Urea Denaturation of Staphylococcal Nuclease Monitored by Fourier Transform Infrared Spectroscopy†

Niels B. From and Bruce E. Bowler*

Department of Chemistry and Biochemistry, University of Denver, 2190 East Iliff Avenue, Denver, Colorado 80208-2436

Received March 18, 1997; Revised Manuscript Received November 21, 1997

ABSTRACT: Fourier transform infrared (FTIR) amide I spectroscopy has not been widely used as a method to study protein folding. Some thorough studies of thermal unfolding have been carried out; however, protein unfolding in the presence of the widely used denaturants guanidine hydrochloride and urea has only recently been reported. Guanidine hydrochloride and urea both absorb strongly in the amide I region, as does H_2O. Here, we have used deuterated ^{13}C-urea as the chemical denaturant and monitored the unfolding transition with deuterium-exchanged staphylococcal nuclease (SNase) in D_2O. These conditions circumvent all subtraction difficulties as the absorption bands of D_2O and denaturant are shifted out of the amide I′ region [Fabian, H., and Manstch, H. H. (1995) *Biochemistry 34*, 13651−13655]. A very reproducible unfolding transition is obtained for SNase. ^{13}C-Urea-induced unfolding of SNase was found not only to be comparable to previous FTIR thermal unfolding data but also to have a denatured-state spectrum similar to those of other thermally denatured proteins. The unfolding is approximately two-state. The infrared spectra in the denatured state show evidence of some residual β-sheet structure as well as other band components not attributable to random structure.

One of the major difficulties in studying the equilibrium between the native and the denatured states of proteins is the relatively low structural resolution of many of the applied techniques. The native-state structure has usually been determined by X-ray crystallography, which serves as a solid structural platform in the investigation. At present, however, no method exists that can give comparable information about the denatured-state conformation of proteins. The alternative is to use a set of different techniques to gather as detailed a picture of the denatured state as possible.

Staphylococcal nuclease (SNase),[1] one of the most studied proteins in the field of protein folding, has been investigated by a large number of techniques and under many different denaturing conditions. Several studies report evidence that the denatured state of this protein is not a true random coil even under severe denaturing conditions (*1*). Fluorescence spectroscopy (*2*) and gel-filtration studies (*3*) on guanidine hydrochloride- (GdnHCl-) denatured SNase, as well as small-angle X-ray scattering on a fragment of the protein that is denatured in the absence of denaturants (*4*), have demonstrated that the degree of expansion of the polypeptide chain is smaller than expected for a random coil polypeptide. Such data suggest a compact denatured state.

To better characterize the denatured state and possible intermediates, new techniques with different strengths must be developed. Two such techniques are currently being optimized toward the needs of protein denaturation investigations: high-resolution NMR (*5*−*7*) and FTIR spectroscopy (*8*−*12*). By applying NMR (*6*, *7*), it has been possible to identify conformations of SNase that remain stable at high concentrations of denaturants. A tentative equilibrium folding pathway for SNase has been proposed on the basis of these experiments.

Infrared spectroscopy can serve as an important complement to NMR results on protein folding. This spectroscopic method is mainly based on absorption due to the carbonyl stretching vibration of the peptide backbone, also known as the amide I band. The frequency of this band depends on the secondary structure of the protein, because the carbonyl stretch vibration is sensitive to the strength of hydrogen bonding in different secondary structures (*13*, *14*). Numerous studies have been devoted to empirical band assignment and quantitative estimation of secondary structure (*15*−*18*). Secondary structure content evaluation by FTIR normally is very close to that found by X-ray diffraction. One of the advantages of using FTIR to study protein folding is the high reproducibility of the spectra, which allows one to detect even minor changes in protein conformation. A gradual change in denaturing conditions can be followed between the well-defined native and the more disordered denatured state, and changes can be assigned to secondary structures. Such data have been obtained for thermal denaturation of proteins (*9*, *12*), and more recently for urea unfolding of ribonuclease A (*8*). Although FTIR spectroscopy presently is unable to give the precise location of a particular secondary structure, and assignment of bands in the amide I region of denatured as well as the native protein can sometimes be problematic, FTIR provides a useful complement to NMR

† This work was supported by NIH Grant GM54281-01 (B.E.B.), by NSF Grant MCB-9304751 (B.E.B.), and by a graduate fellowship from the Colorado Institute for Research in Biotechnology (N.B.F.).

* Corresponding author.

[1] Abbreviations: SNase, staphylococcal nuclease; GdnHCl, guanidine hydrochloride; FSD, Fourier self-deconvoluted; amide I, infrared absorbance due mainly to the carbonyl of the peptide bonds of a protein; amide I′, same infrared absorbance as amide I except protein amides have been deuterated and the spectrum is acquired in D_2O.

S0006-2960(97)00620-X CCC: $15.00
Published on Web 01/22/1998

since it is not subject to the structural averaging problems inherent in NMR. Thus, a global picture of the denatured-state structure is possible. Thermal denaturation of three different proteins has shown very similar denatured states upon resolution enhancement (9, *10*, *12*, *19*): a major peak around 1644 cm^{-1}, which is assigned to random coil structure, and a major shoulder in the high wavenumber range, at frequencies normally assigned to turn and β-sheet structure. Data presented here further confirm this observation for urea-denatured SNase.

Fabian and Mantsch (*10*) demonstrated that an IR spectrum of ribonuclease A could be obtained in 8 M urea using deuterated ^{13}C-urea and deuterated protein in D_2O. More recently, the complete equilibrium unfolding of this protein has been monitored by this method (*8*). With deuterated ^{13}C-urea in D_2O, the denaturant and water absorption bands shift away from the amide I region, overcoming the subtraction problems normally associated with infrared studies of solvent denaturation (*11*). We have applied these methods to SNase because it presents an interesting case to test the abilities of FTIR spectroscopy to elucidate the subtleties of protein folding. We have also extended the methodology by using Fourier self-deconvolution enhancement techniques coupled to curve-fitting analysis to allow the behavior of individual components of the amide I′ band to be assessed during denaturation. There is much discussion regarding the participation of intermediates (*20*) versus residual denatured-state structure (*21*) in the folding pathway of this protein. Although the unfolding of SNase appears to be two-state according to our FTIR analysis, the data presented here provide additional evidence for the presence of residual structure after the main unfolding transition of SNase. Some inferences into the nature of this residual structure can also be obtained from the frequencies of the components of the amide I′ band that remain in 6 M urea.

Calorimetric studies have suggested for a number of variants of SNase that an intermediate may be formed during unfolding and may be responsible for the observed changes in *m*-values derived from GdnHCl denaturation (*20*). This intermediate is believed to involve loss of the α-helix structure of SNase, leaving predominately β-sheet structure. It is difficult to monitor β-sheet directly with most existing methods. However, due to transition dipole coupling (*22*), the main frequency for β-sheet in the amide I region is shifted well away from those due to other types of secondary structure (*8*). For SNase the loss of the main β-sheet band is easily monitored by FTIR, which should provide a direct method for determining the presence of β-sheet intermediates in future studies.

MATERIAL AND METHODS

Protein Preparation. Wild-type SNase was prepared from *Escherichia coli* strain AR120 kindly provided by Dr. David Shortle (The John Hopkins University). The protein was purified as previously described (*23*). Protein purity was monitored by Coomassie Brilliant Blue stained SDS−PAGE and was estimated to be at least 95%. Protein concentration was determined using an A_{280} value of 0.93 for a 1 mg/mL solution of SNase. Urea concentrations were determined by refractive index measurements against buffer (*24*). All experiments were performed in a 25 mM sodium phosphate and 100 mM sodium chloride buffer. Deuterated ^{13}C- and ^{12}C-urea were prepared by repeated lyophilization from excess D_2O. ^{13}C-urea was obtained from Sigma. H/D exchange of the protein was carried out for 30 min at pH/D 10.5 in D_2O. The pH was then lowered to 7 and ions were removed by repeated concentration and refilling with D_2O in a Centricon-3 ultrafiltration device. Urea denaturation data were collected at pH 7. H → D exchange was considered complete due to the shift of the amide II band (see Figure 1) and the absence of any amide A band resulting from an N−H stretch near 3280 cm^{-1} (*22*).

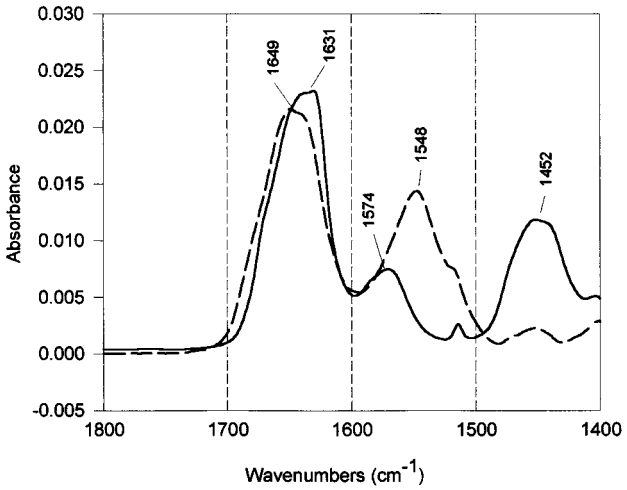

FIGURE 1: IR spectra of the amide I (I′) and II (II′) bands of staphylococcal nuclease in H_2O and deuterated in D_2O. The signal-to-noise ratio of the amide I (I′) band was 2800:1 in D_2O and 1300:1 in H_2O. The path length is 6 μm and the concentration is 20 mg/mL. (—) SNase in D_2O; (- - -) SNase in H_2O.

CD Spectroscopy. Unfolding of SNase, as a function of the concentration of ^{12}C-urea, or of deuterated ^{12}C-urea, was monitored by CD spectroscopy as the difference in ellipticity between 220 and 250 nm ($\theta_{220} - \theta_{250}$). Measurements were made with a Jasco 500C spectropolarimeter using a time constant of 2 s, a sensitivity of 5 mdeg/cm, and a slit width of 1800 μm. The protein concentration was approximately 45 μg/mL (cell path length was 10 mm) for urea unfolding. Unfolding was carried out as described previously (*25*). Measurements were made at 20 ± 0.1 °C using a Neslab Model RTE 5 circulating bath and a jacketed CD cell. Standard procedures that have been described previously (*24*, *26*) were used to evaluate the denaturation data.

FTIR Spectroscopy. IR spectra were collected at 20 °C on a Nicolet Magna 550 IR spectrometer (equipped with a Hg/Cd/Te detector) continuously purged with nitrogen. Samples were loaded in a Beckman FH-01 cell with CaF_2 windows and a 6 μm path length spacer. A total of 256 scans were recorded per spectrum in a single-beam mode at a resolution of 2 cm^{-1}. Protein concentration was kept constant in a given experiment but varied between 20 and 25 mg/mL in different experiments. Typically, the signal-to-noise (S/N) ratio was 2800:1 in D_2O samples. At 6 M ^{13}C-urea a slightly lower concentration of 15 mg/mL was used. FTIR sample preparation was performed as previously described (*11*).

Analysis of IR Spectra. Deuteration of ^{13}C-urea shifts the major urea absorption band from 1624 cm^{-1} to 1562 cm^{-1} (*8*, *10*), leaving only a slight overlap with the amide I′ band.

An over- or undersubtraction of the denaturant spectrum was found not to interfere with the amide I′ band shape above 1620 cm^{-1} and not to change the resolution-enhanced spectra. However, an inaccurate subtraction can change the overall area of the amide I′ absorption band. To be able to compare amide I′ areas and possible changes in absorptivity due to denaturation, an accurate subtraction procedure must be performed (*11*). First, buffer was subtracted using the 1209 cm^{-1} band due to D_2O as a reference. Next, a background spectrum of the same molarity of ^{13}C-urea was subtracted, keeping the relative intensities of the amide I′ and amide II′ bands approximately the same in the final spectrum. Finally, water vapor was removed by subtraction (*27*).

To be able to compare the amide I′ absorption area at different urea concentrations, a subtraction was carried out such that the featureless region of the spectrum between 2100 and 1750 cm^{-1} had an absorbance of zero. This essentially amounted to subtracting a constant absorbance from the entire spectrum. By performing baseline correction in this way all peak shapes and relative sizes are unaffected. This method of baseline correction is preferable to one in which the baseline is simply drawn from an absorbance of zero near the high-energy edge of the amide I′ band to the saddle between the amide I′ and the carboxylate side chain absorbance. This latter procedure causes loss of real amide I′ intensity that is biased toward the low-energy portion of the amide I′ band. In our procedure, overlap of the low-energy region of the amide I′ spectrum with the adjacent absorbance band of the carboxylate side chains is taken care of in subsequent curve-fitting of Fourier self-deconvoluted spectra.

After subtraction was accomplished, band-narrowing was performed by Fourier self-deconvolution (FSD) and second-derivative methods (*17*). In native-state spectra, peak positions and areas were obtained by curve-fitting FSD-enhanced spectra with Gaussian band profiles. For all spectra, the enhancement factor was kept well below log (S/N) as suggested previously (*28*). Initially, a resolution enhancement factor of 3.3 and a bandwidth at half-height of 19.6 cm^{-1} were used. These bands were then imported into less enhanced FSD spectra (resolution enhancement factor of 2.4 and bandwidth at half-height of 15.5 cm^{-1}), band positions were fixed, and iteration was continued until convergence between the fitted and actual spectra was obtained. By visual inspection the fitted and the original spectra appeared identical.

To follow changes in the spectra due to a gradual increase in denaturing conditions, second-derivative methods were applied to baseline-adjusted amide I′ bands and are shown without further manipulation. The denaturation transition was also monitored by FSD enhancement as described for the native-state spectra with an enhancement factor of 2.4 and a bandwidth at half-height of 15.5 cm^{-1}. Curve-fitting was performed by importing bands from less denatured curve-fitted spectra and iterating with fixed band positions until the solution was at a minimum or the spectra converged. Bands hitting lower limitations for height or width were deleted during the fitting procedure. Peak positions where a deviation could be observed between the actual and the fitted spectra were allowed to float in the final set of iterations in the curve-fitting procedure. Typically, peak positions shifted by less than 1 cm^{-1}.

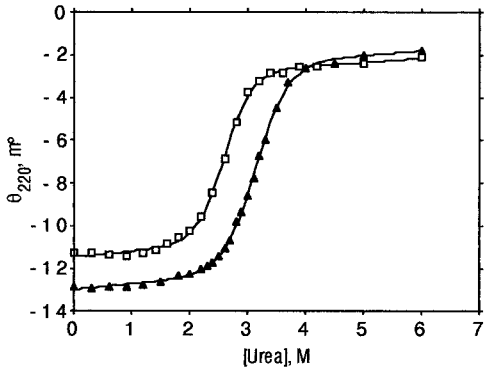

FIGURE 2: ^{12}C-Urea unfolding curves for SNase and deuterated SNase in H_2O and D_2O monitored by CD spectroscopy. Deuteration causes a shift in the midpoint of unfolding from 2.65 M urea in H_2O to 3.1 M urea in D_2O. (▲) SNase in D_2O; (□) SNase in H_2O. Solid lines represent nonlinear least-squares fits to a two-state unfolding transition as previously described (*26*). $\Delta G°_u{}^{H_2O}$ ($\Delta G°_u{}^{D_2O}$) and *m*-values obtained are given in the text.

RESULTS

Native-State Spectra in H_2O and D_2O. Figure 1 shows the amide I band of SNase in H_2O and the amide I′ band of deuterated SNase in D_2O. Complete deuteration was accomplished by increasing the pH in the protein solution to 10.5 for 30 min. No batch to batch variations were observed in the amide I′ and amide II′ band position, shape, and size, indicating that a complete deuteration has been accomplished. The deuteration causes, as expected (*17*, *29*), an approximately 10 cm^{-1} shift of the amide I band center as well as a change in the band shape. The amide II band, which is ascribed to an in-plane-bending vibration of N−H in combination with C−N stretching (*22*), experiences a much more severe shift from approximately 1548 cm^{-1} to approximately 1452 cm^{-1}. A peak at approximately 1574 cm^{-1} is revealed when the amide II band shifts; this peak is assigned to the carboxylate stretching vibration of aspartate and glutamate side chains (*30*). The loss of the amide II band at 1548 cm^{-1} is complete, indicating a full deuteration of the amide nitrogens. The tyrosine ring vibration at 1515 cm^{-1} (30), which is only a shoulder on the amide II band, is baseline-resolved in the spectrum of the deuterated protein.

The influence that H/D exchange has on the structural properties of a protein is not fully understood but the exchange could possibly alter the protein stability as well as its structure. The CD results show a significant increase in the unfolding midpoint of the protein from 2.65 ± 0.06 M urea in H_2O to 3.10 ± 0.06 M urea in D_2O (Figure 2). However, the *m*-value in D_2O [2.08 ± 0.01 kcal/(mol·M)] is smaller than in H_2O [2.34 ± 0.18 kcal/(mol·M)], such that the stability of SNase in D_2O ($\Delta G°_u{}^{D_2O} = 6.45 \pm 0.13$ kcal/mol) is only slightly higher than in H_2O ($\Delta G°_u{}^{H_2O} = 6.17 \pm 0.33$ kcal/mol). Calorimetric studies of several proteins in H_2O and D_2O indicate that differences in hydrophobic hydration in D_2O versus H_2O account for almost all of the effects of deuteration on the thermodynamics of protein folding (*31*). An evaluation of changes in structural features in the native state due to deuteration can be made by estimating the secondary structure distribution of the deuterated and nondeuterated proteins by curve-fitting FSD spectra of the protein (Figure 3). From the band assignment data of Dong and Caughey (*29*) for H_2O and of Byler and

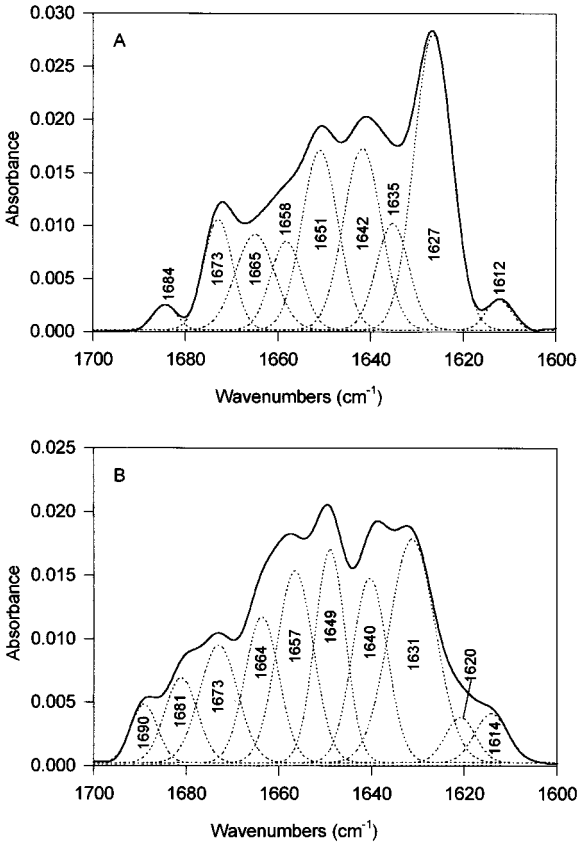

FIGURE 3: (A) Curve-fitted Fourier self-deconvoluted amide I′ band of SNase in D_2O with a half-bandwidth of 15.5 cm^{-1} and an enhancement factor of 2.4. (B) Curve-fitted Fourier self-deconvoluted amide I band of SNase in H_2O with a half-bandwidth of 17.2 cm^{-1} and an enhancement factor of 2.5. (—) Original spectra; (•••) curve-fitted bands.

Table 1: Secondary Structure Assignment of SNase in D_2O and H_2O

(A) Curve-Fitted Band Positions and Percent Areas of FSD-Enhanced SNase Spectra in H_2O and D_2O, Along with Empirical Secondary Structure Assignments

H_2O			D_2O		
band position (cm^{-1})	assignment[a]	area (%)	band position (cm^{-1})	assignment[b]	area (%)
1689.1	β strand	3.6	1684.3	turn	1.5
1681.1	turn	6.3	1672.9	turn/β strand	8.4
1672.9	turn	10.3	1664.9	turn	9.7
1663.6	3_{10} helix	11.2	1658.2	3_{10} helix	7.2
1656.5	α helix	15.9	1650.9	α helix	16.9
1648.9	random	14.7	1641.7	random	17.9
1640.3	β strand	14.5	1635.2	β strand	8.9
1631.2	β strand	23.5	1626.5	β strand	28.8

(B) Comparison of SNase Secondary Structure Distribution by IR in H_2O and D_2O with Data from X-ray Crystallography

	X-ray[c] (%)	H_2O (%)	D_2O (%)
β-sheet	38.7	41.6	41.9
helix	26.8	27.1	24.1
turn		16.6	15.4
unordered		14.7	17.9

[a] Assignment from Dong and Caughey (*29*). [b] Assignment from Susi and Byler (*15*). [c] Assignment from Levitt and Greer (*33*).

Susi (*15*) for D_2O, comparable secondary structure estimations are found in the deuterated and nondeuterated protein (Table 1). The values reported here are consistent with previous infrared work on SNase (*12*, *32*). The infrared

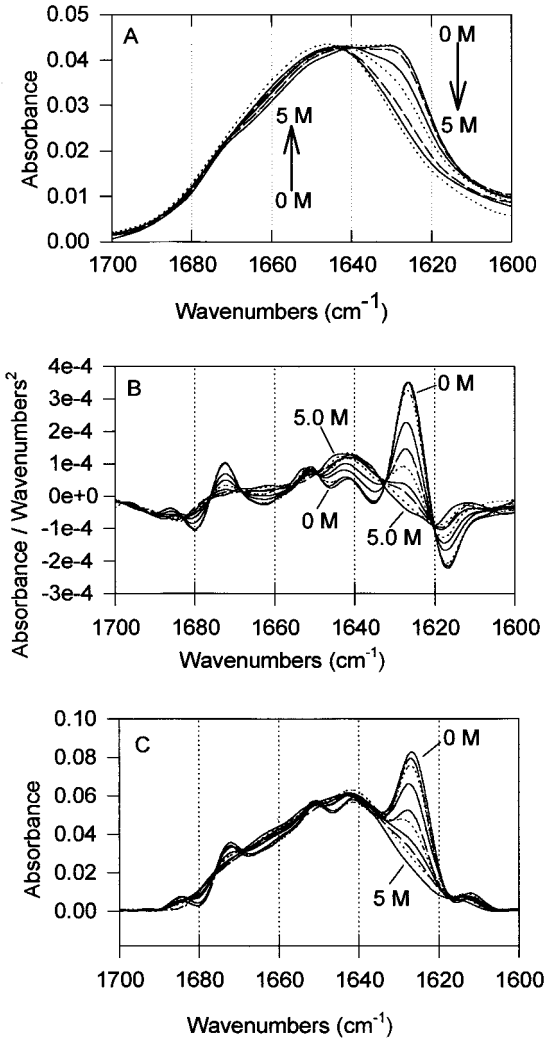

FIGURE 4: (A) IR spectra of the amide I′ band between 0 and 5 M urea in D_2O. To facilitate comparison between different urea concentrations, any offset in baseline was corrected by setting the flat 2100−1750 cm^{-1} range to 0 absorbance and adjusting the entire spectrum accordingly. (—) 0, 2.5 and 4.0 M; (•••) 1.0, 2.8, and 5.0 M; (- - -) 2.0 and 3.2 M. (B) Second-derivative IR spectra of the amide I′ region of SNase between 0 and 5 M urea. Seven crossover points are observed. (—) 0, 2.5, 3.2, and 5.0 M; (- - -) 1.0, 2.8, and 3.4 M; (•••) 2.0, 3.0, and 4.0 M. (C) FSD-enhanced spectra of the amide I′ region of SNase between 0 and 5 M urea. (—) 0, 2.5, 3.2, and 5.0 M; (- - -) 1.0, 2.8, and 3.4 M; (•••) 2.0, 3.0, and 4.0 M.

secondary structure assignment is also consistent with the assignment of Levitt and Greer (*33*) using X-ray data for SNase (Table 1). We therefore believe that the results show no evidence of conformational change due to deuteration of SNase. NMR studies on the ternary complex (Ca^{2+}, pdTp) of SNase show that NOE interactions obtained in H_2O and D_2O solution are consistent with the same structure (*34*−*37*).

Urea Unfolding in D_2O Monitored by FTIR. Figure 4A illustrates the changes in the amide I′ band for SNase due to ^{13}C-urea denaturation in D_2O. A gradual change toward a more symmetrical band, centered around the frequency normally assigned to random coil (*29*), is observed. The changes in the amide I′ band occur with an approximate isosbestic point near 1640 cm^{-1} indicating that the unfolding of SNase approximates a two-state transition. However, the isosbestic point is not clean, which could suggest some deviation from two-state behavior. It is likely that the lack

of a perfect isosbestic point results from small inaccuracies in subtraction of the ^{13}C-urea absorption band in different spectra. Inspection of separate unfolding experiments is consistent with this possibility. Therefore, there is no compelling reason to suggest that this transition is not two-state. Substantial loss in absorption occurs between 1640 and 1600 cm^{-1}. However, this loss is partially compensated by an increase in absorption above 1640 cm^{-1}, which leads to an overall loss in band area of approximately 10%. Heat denaturation of SNase results in a comparable change in the amide I′ band shape (*12*) and a comparable transition in the second-derivative resolution-enhanced spectra. Xie et al. (*12*), however, report a 28% decrease in the amide I′ band area during thermal unfolding. A large decrease in the amide I′ area below 1640 cm^{-1} with no increase above 1640 cm^{-1} was observed, in contrast to our urea denaturation results. The source of these differences is unclear, but they may indicate differences in the final denatured state. For urea unfolding, the small decrease in absorptivity as a function of decreasing amounts of structured conformation indicates that the absorption coefficient of the C═O stretch vibration is somewhat dependent on protein structure. This relatively small decrease in the amide I′ extinction coefficient upon denaturation, however, should have only a small impact on quantitative assessment of the denaturation process by curve-fitting procedures.

To obtain more detailed information regarding structural changes during denaturation, resolution enhancement was performed on all spectra using second-derivative methods. Figure 4B shows the unmanipulated second-derivative spectra as a function of increasing urea concentrations. Between 0 and 2 M urea virtually no changes occur in the second-derivative spectra, which is in good agreement with CD data, where less than 5% of the ellipticity has been lost by 2 M urea (see Figure 2). Between 2.5 and 3.5 M urea, a cooperative transition occurs with smooth changes in the height of the second derivative in seven resolvable amide I′ band components separated by seven crossover points. If the change in the magnitude of the second derivative is monitored as a function of urea concentration at the 1626.3, 1641.7, 1652.0, and 1672.1 cm^{-1} components, the changes in magnitude occur essentially in parallel during the unfolding transition (Figure 5). In CD experiments (Figure 2), loss in ellipticity continues after the main unfolding transition. IR spectroscopy also shows this small postunfolding change in secondary structure as a further loss in the component near 1630 cm^{-1} and an increase in the component near 1660 cm^{-1} (see Figure 4B). This postunfolding change in the infrared spectrum can also be seen in the original amide I′ absorption band (see Figure 4A). As was the case for the changes in the original amide I′ absorption band, the changes in the second-derivative enhanced spectra during the urea denaturation process qualitatively resemble what was observed for heat denaturation (*12*).

Second-derivative resolution enhancement provides a relatively user-neutral means of deconvoluting amide I infrared spectra. Unfortunately, the magnitude of the second derivative depends on the sharpness of the component bands underlying the amide I′ absorbance envelope (*14*). Thus, following the height of second-derivative components will not accurately quantitate changes in structure as a protein unfolds. For quantitative purposes, the unfolding transition

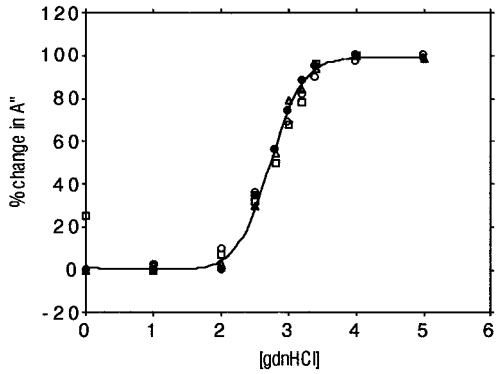

FIGURE 5: Magnitude of the second derivative presented in Figure 4B at four wavelengths covering the breadth of the amide I′ band, shown as a function of the concentration of urea. Symbols are as follows: (○) 1626.3 cm^{-1}; (△) 1641.7 cm^{-1}; (□) 1652.0 cm^{-1}; (●) 1672.1 cm^{-1}. The solid curve has no theoretical significance; it is meant only to guide the eye. The percent change in the second derivative is $(A'' - A''_{min})/(A''_{max} - A''_{min})100$ at wavelengths which increase in magnitude during unfolding and $(A''_{max} - A'')/(A''_{max} - A''_{min})100$ at wavelengths that decrease in magnitude during unfolding. A'' is the magnitude of the second derivative at a given concentration of urea, A''_{max} is the maximal magnitude of the second derivative and A''_{min} is the minimum magnitude of the second derivative.

can be monitored by changes in the original amide I′ band or by curve-fitting FSD enhanced spectra. With an FSD enhancement factor of 2.4 and a half-bandwidth of 15.5 cm^{-1}, the decrease in the area of the amide I′ band envelope due to denaturation is very close to what is observed for the amide I′ band itself (about 10%). Higher enhancement factors lead to larger decreases in the area of the amide I′ band during denaturation, thus presenting problems for quantitation as with the second derivative. The FSD-enhanced spectra show a similar gradual loss in intensity in some band components and an increase in others during the unfolding transition as observed with the second derivative (Figure 4C). A number of approximate isosbestic points are observed, near the frequencies of the crossover points in the second-derivative enhanced spectra, indicating that similar band components are being monitored by the two methods of resolution enhancement. To quantify the unfolding process, bands from curve-fitting were generated using the assumption that band components change gradually in size and shape and to a lesser extent in frequency during the denaturation process (see Materials and Methods). Since denaturation appears to be a process of smooth change in band components (Figures 4B and 5), initial parameters for fitting each FSD-enhanced spectrum in the denaturation were taken from the final fit to the previous urea concentration. Figure 6 shows the curve-fitted FSD-enhanced amide I′ band at four illustrative concentrations, with Figure 3A showing the initial bands at 0 M urea. A gradual change in band size and shape is seen toward fewer and wider bands. At 6.0 M urea the curve-fitted spectrum is very similar to the curve-fitted FSD-enhanced spectrum of the heat-denatured state of RNase T1 (*9*) with a major peak at 1642 cm^{-1} ascribed to random structure and two major peaks in the high-frequency range, a region normally attributed to turn structure. Figure 7 shows a comparison between the CD data and percent changes in the intensity of the original amide I′ absorbance band at 1630 cm^{-1} as well as the percent changes in the areas of the band components at 1627 and 1642 cm^{-1} obtained from FSD

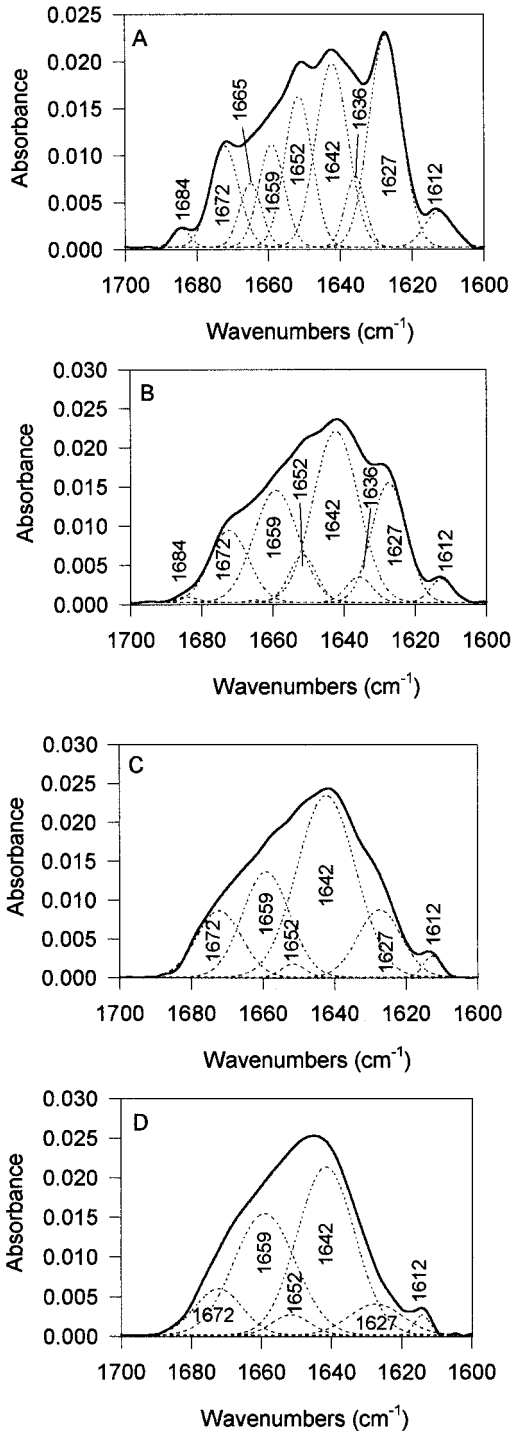

FIGURE 6: Curve-fitted FSD-enhanced spectra of the amide I′ region of SNase. Four illustrative concentrations of the denaturation transition are shown. (—) Original spectra; (- - -) curve fitted bands. (A) 2.5 M urea; (B) 3.0 M urea; (C) 3.4 M urea; (D) 6.0 M urea.

curve-fitting analysis. The IR data indicate a somewhat lower unfolding midpoint urea concentration than the CD results, the effect being most pronounced for the amide I′ absorbance band monitored at 1630 cm^{-1} ($C_{1/2}$ = 2.8 M urea versus 3.1 M urea for CD data). The area of the 1642 cm^{-1} band decreases after 4 M urea, consistent with the previously mentioned shift toward the higher frequency region in the unmanipulated absorbance data (Figure 4A). The FSD component bands at 1627 and 1642 cm^{-1} follow the CD transition more closely ($C_{1/2}$ = 2.95 and 2.94 M urea, respectively) than the unenhanced band; however, they still precede the CD-monitored transition. The different components, representing diverse secondary structures within the protein, monitored by FTIR, track closely together (Figures 5 and 7). Since the amide I band monitors all the peptide bonds in the protein, this synchronicity strongly argues for a two-state process. The deviation from the CD data may be due to the substantial difference in protein concentration (~2 μM for CD, ~1 mM for FTIR) used in the two experiments.

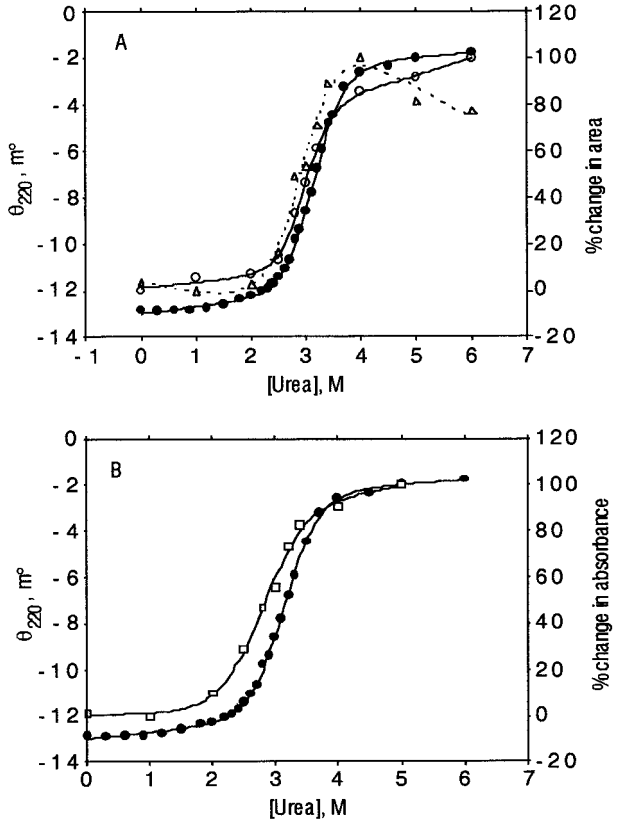

FIGURE 7: Comparison between SNase ^{13}C-urea denaturation monitored by CD and FTIR. (A) Percent change in the FSD component band areas at 1627 cm^{-1} (○) and 1642 cm^{-1} (△) as a function of urea concentration compared to the ellipticity from CD data (●) as a function of urea concentration. (B) Percent change in the absorbance at 1630 cm^{-1} (□) as a function of urea concentration compared to CD data as in panel A. For IR data the % change in area or absorbance is $(A - A_{min})/(A_{max} - A_{min})$x100 for band components that increase in area or absorbance during unfolding and $(A_{max} - A)/(A_{max} - A_{min})$100 for band components that decrease in area or absorbance during unfolding. A is the area or absorbance of the band at a given concentration of urea, A_{max} is the maximal area or absorbance of the band, and A_{min} is the minimum area or absorbance of the band. The lines in panels A (solid for CD data and 1627 cm^{-1} FSD component, dotted for 1642 cm^{-1} FSD component) and B represent nonlinear least-squares fits of the data to a two-state unfolding model as described previously (*26*). The midpoint urea concentrations for the unfolding transitions, $C_{1/2}$, derived from these fits are given in the text.

DISCUSSION

FTIR amide I spectroscopy has not been widely used as a method to study protein folding. Some thorough studies of thermal (*9*) and urea (*8*) unfolding by FTIR have been carried out, and preliminary work on protein unfolding in the presence of the widely used denaturant GdnHCl (*11*) has been reported. Infrared amide I spectroscopy has some real

advantages versus other commonly used methods. Since the amide I band reports on all of the peptide carbonyls in the protein, the method can in principle monitor the unfolding process for all parts of the protein simultaneously. Thus, if changes occur synchronously throughout the breadth of the amide I band, the unfolding of the protein is two-state. Methods such as tryptophan fluorescence may only monitor unfolding in the immediate vicinity of the probe tryptophan (*38*) and the large differences in molar ellipticity for different types of secondary structure tend to bias circular dichroism toward monitoring loss of α-helical structure. Our data for the urea denaturation of SNase indicate only a small loss in the extinction coefficient of the amide I′ band associated with denaturation, suggesting that only relatively small differences in extinction coefficient exist for different types of protein secondary structure. Reports exist of changes in extinction coefficient as large as 30% due to changes in secondary structure (*14*), which suggests that some secondary structure bias could occur. However, relative to other spectroscopic probes this is a small effect, and thus infrared amide I spectroscopy appears to offer the potential to follow protein unfolding with little bias throughout the entirety of a protein's sequence. Given the recent interest in the role of intermediates in the unfolding of proteins (*20*), FTIR should be a useful tool.

Second-derivative methods (*16*) and Fourier self-deconvolution (*28*) permit substantial deconvolution of the amide I band, and therefore the loss of different types of secondary structure during unfolding can be followed separately. Our data indicate that this is most straightforward for turn and β-sheet structures. Unfortunately, random structure and α-helix structure have amide I components that are fairly close to each other and thus their contributions are more difficult to deconvolute reliably, at least in the case of SNase.

The main problem with using FTIR spectroscopy to follow protein folding is the coincidence of the amide I absorption band with the IR absorption bands of urea and GdnHCl in water. Previous work with denaturation in GdnHCl (*10*) indicated that, at wavenumbers above 1660 cm^{-1}, accurate subtraction of the GdnHCl absorbance was difficult. We attempted to follow the denaturation of SNase by GdnHCl in H_2O quantitatively; however, the results were disappointing. Although the loss of the β-sheet band near 1631 cm^{-1} could be observed reliably, the reproducibility in the high-wavenumber region was too poor for quantitative work, particularly at GdnHCl concentrations of 1.5 M or higher. However, the complete unfolding transition could be monitored in the β-sheet region and gave data consistent with CD-monitored unfolding of SNase.

Studies with ^{13}C-urea in H_2O lead to similar problems. The ^{13}C label shifts the urea infrared absorbance to 1624 cm^{-1} in H_2O. However, a significant, high-wavenumber shoulder extends well into the amide I region. In this case, we had significant subtraction problems in the low-wavenumber region of the amide I band at urea concentrations above 2.6 M. This situation prevented complete monitoring of the urea unfolding transition. Fortunately, it has been demonstrated recently that the infrared absorbance of deuterium-exchanged ^{13}C-urea is shifted to 1562 cm^{-1} (*8*, *10*). This has allowed the highly reproducible, quantitative assessment of SNase unfolding presented here to be achieved.

Using CD methods, we have demonstrated that SNase is more stable to urea denaturation in D_2O than in H_2O. It is of concern that complete deuterium exchange could alter the native structure of the protein, and thus the unfolding process being followed in D_2O versus H_2O might be different. Secondary structure analysis in H_2O and D_2O (see Table 1) gave similar results, and therefore such an effect appears not to be a concern. Thus, we are confident that D_2O as a solvent does not cause a substantial perturbation to the unfolding process being monitored, although differences in the hydrophobic effect in D_2O versus H_2O may affect the absolute values of $\Delta G^\circ_{u}{}^{H_2O}$ ($\Delta G^\circ_{u}{}^{D_2O}$) observed (*31*).

Our infrared data for urea denaturation of SNase indicate that unfolding of the wild-type protein is best described as a two-state process. The lack of a clean isosbestic point during the unfolding transition in the raw absorbance data most likely reflects small inaccuracies in subtraction of ^{13}C-urea and not a deviation from two-state behavior (Figure 4A). The synchronous loss and gain in intensity of several of the underlying band components (Figures 4B and 5) also supports a two-state process. An advantage of the infrared experiment is that it monitors all peptide bonds in the protein. Thus, synchronous change in the underlying components of the band indicates that diverse secondary structures throughout the protein are being lost simultaneously. Data obtained under similar pH and salt conditions by calorimetry (*39*), urea-gradient gel electrophoresis (*40*), and CD and tryptophan fluorescence (*23*) also indicate two-state behavior for wild-type SNase.

The loss of β-sheet structure monitored by a decrease in the intensity of the amide I′ spectrum near 1630 cm^{-1} is the most prominent change in the FTIR spectrum of SNase during denaturation by deuterated ^{13}C-urea (Figure 4). The observation that loss of β-sheet structure is almost coincident with loss of α-helix structure, as monitored by CD spectroscopy, supports two-state unfolding of this protein. The ability to monitor loss of β-sheet relatively unambiguously, should be particularly useful for future studies with variants of SNase that have significant changes in *m*-values relative to the wild-type protein. Calorimetric studies have indicated the presence of intermediates for these variants and an intermediate composed mainly of β-sheet has been proposed (*20*).

In our FTIR data, there appears to be evidence for a noncooperative change in the structure after the main unfolding transition at high urea concentrations (Figures 4A and 6). This noncooperative loss of structure is not observed calorimetrically (*38*), although CD data are consistent with small structural changes after the main cooperative unfolding transition (Figure 2). Of particular interest is a consideration of whether significant residual structure can be detected in amide I′ spectra obtained after the cooperative unfolding transition (4 M urea and above). It is clear that a small amount of β-sheet structure remains at 4 M urea (see Figure 7A) and is slowly lost as the concentration of urea is increased to 6 M. This change in β-sheet parallels a continued loss in ellipticity observed after 4 M urea (see Figure 2). Similar behavior is also observed for changes in the CD spectrum of a 131 amino acid fragment of SNase. Between 4 and 6 M urea, ellipticity attributable to β-sheet structure is lost (*6*). At 4 M urea the NMR data of Wang and Shortle (*6*) suggest that the β-sheets, β2 and β3 are still

populated, which would require ~10% β-sheet content at 4 M urea. Our infrared data indicate a total β-sheet content of 10.7% at 4 M urea, decreasing to 7.6% at 6 M urea. These data are clearly consistent with noncooperative loss of residual structure from the denatured state after the major cooperative unfolding transition. It should be noted that our infrared data were obtained with fully intact SNase whereas Wang and Shortle (*6*) used a 131 amino acid fragment of the protein that does not fold to the native state even in water. Thus, the two systems give qualitatively the same result.

Even under strongly denaturing conditions (6 M urea), the amide I′ absorption band does not collapse to a completely symmetric random coil spectrum (Figure 6D). The major band component is found at 1642 cm^{-1} (44.7% of the total amide I′ band area), which has been attributed to random coil by empirical methods (*15*, *29*). Two other significant components are found at 1659 cm^{-1} (34.5% of total band area) and 1672 cm^{-1} (9.7% of total band area). Studies of the heat-denatured state of proteins in D_2O by IR have shown spectra qualitatively similar to this spectrum (9, *12*, *19*): a peak centered around 1644 cm^{-1} and a shoulder in the high-frequency range. Torii and Tasumi (*41*) calculated that non-α and non-β structure in folded proteins can spread over a wide wavenumber region, suggesting that the protein conformations causing this high-energy shoulder could be unordered or turn structures. However, we are observing this shoulder in a denatured protein, and it must be kept in mind that a major factor in determining the frequency of the amide I band is hydrogen bonding. For cyclic peptides in D_2O, carbonyls not involved in intramolecular hydrogen bonds have been assigned to absorbances between 1640 and 1655 cm^{-1}. These carbonyls are assumed to hydrogen-bond to the D_2O solvent (*42*, *43*). On the basis of this precedent, it seems reasonable that the major band at 1642 cm^{-1} and possibly the smaller band at 1659 cm^{-1} in the 6 M urea spectrum are due to randomly structured carbonyls hydrogen-bonded to the D_2O solvent. It is interesting to note that the 1642 cm^{-1} FSD component loses intensity above 4 M urea (Figure 7A) largely at the expense of the band at 1659 cm^{-1}. CD experiments of Tiffany and Krimm (*44*) indicate an interaction of urea with the peptide backbone that increases with urea concentration. On this basis, we tentatively suggest that the band at 1659 cm^{-1} could be due to hydrogen bonding of randomly structured peptide carbonyls to deuterated urea.

The band observed at 1672 cm^{-1} is more perplexing. Heat-denatured proteins that aggregate in the denatured state typically give a pair of bands, one near 1618 cm^{-1} and the other near 1685 cm^{-1} (*45*, *46*). Thus, it seems unlikely that this band is attributable to aggregation. Only carbonyls that are conformationally distorted or in a low dielectric environment are expected to have frequencies in this region (*13*, *14*). Thus, we tentatively suggest that a portion of the denatured state of SNase is involved in a hydrophobic clusterlike structure with a low dielectric or has peptide bonds in conformationally restricted environments. H/D exchange NMR studies on SNase in urea are consistent with some regions of residual structure being involved in hydrophobic clusters rather than stable hydrogen-bonded structure (*7*). This structural assignment from NMR data is consistent with the interpretation proposed for the high-wavenumber shoulder in the amide I′ IR spectrum of SNase at 6 M urea.

CONCLUSION

We have demonstrated that use of deuterium-exchanged ^{13}C-labeled urea allows the complete unfolding transition of SNase to be monitored by amide I′ infrared spectroscopy. The spectra are highly reproducible and can be obtained at high signal-to-noise ratios. Under these conditions, individual components of the absorbance band can be deconvoluted, allowing the loss and gain of different types of secondary structure to be followed during denaturation. Changes in β-sheet structure produce the most prominent effects. Data for SNase are consistent with a two-state transition under the buffer and pH conditions used for urea unfolding. The main transition is followed by a noncooperative loss of structure. The urea-denatured state of SNase appears to have a significant amount of random structure. A small amount of hydrogen-bonded sheet remains at 4 M urea at the end of the cooperative unfolding transition and is slowly lost with increasing urea concentration. A shoulder in the high-energy region of the amide I′ band is observed at 6 M urea that is tentatively assigned to hydrophobic clusters in which the main-chain carbonyl is shielded from hydrogen bonding to solvent. This high-energy shoulder appears to be a common feature in the infrared spectra of denatured proteins.

ACKNOWLEDGMENT

We thank John Carpenter at the Pharmacy School, University of Colorado Health Sciences Center, for generous use of his infrared spectrometer.

REFERENCES

1. Dill, K. A., and Shortle, D. (1991) *Annu. Rev. Biochem. 60*, 795−825.
2. James, E., Wu, P. G., Stites, W., and Brand, L. (1992) *Biochemistry 31*, 10217−10225.
3. Shortle, D., and Meeker, A. K. (1989) *Biochemistry 28*, 936−944.
4. Flanagan, J. M., Kataoka, M., Shortle, D., and Engelman, D. M. (1992) *Proc. Natl. Acad. Sci. U.S.A. 89*, 748−752.
5. Neri, D., Billeter, M., Wider, G., and Wuthrich, K. (1992) *Science 257*, 1559−1563.
6. Wang, Y., and Shortle, D. (1995) *Biochemistry 34*, 15895−15905.
7. Wang, Y., and Shortle, D. (1996) *Protein Sci. 5*, 1898−1906.
8. Reinstadler, D., Fabian, H., Backmann, J., and Naumann, D. (1996) *Biochemistry 35*, 15822−15830.
9. Fabian, H., Schultz, C., Naumann, D., Landt, O., Hahn, U., and Saenger, W. (1993) *J. Mol. Biol. 232*, 967−981.
10. Fabian, H., and Mantsch, H. H. (1995) *Biochemistry 34*, 13651−13655.
11. Bowler, B. E., Dong, A., and Caughey, W. S. (1994) *Biochemistry 33*, 2402−2408.
12. Xie, L., Jing, G.-Z., and Zhou, J.-M. (1996) *Biochim. Biophys. Acta 328*, 122−128.
13. Jackson, M., and Mantsch, H. H. (1991) *Can. J. Chem.* 69, 1639−1642.
14. Jackson, M., and Mantsch, H. H. (1995) *CRC Crit. Rev. Biochem. Mol. Biol. 30*, 95−120.
15. Byler, D. M., and Susi, H. (1986) *Biopolymers 25*, 469−487.
16. Susi, H., and Byler, D. M. (1986) *Methods Enzymol. 130*, 290−311.
17. Surewicz, W. K., and Mantsch, H. H. (1988) *Biochim. Biophys. Acta 952*, 115−130.
18. Dong, A., Huang, P., and Caughey, W. S. (1990) *Biochemistry 29*, 3303−3308.
19. Seshadri, S., Oberg, K. A., and Fink, A. L. (1994) *Biochemistry 33*, 1351−1355.

20. Privalov, P. L. (1996) *J. Mol. Biol. 258*, 707−725.
21. Shortle, D., Wang, Y., Gillespie, J. R., and Wrable, J. O. (1996) *Protein Sci. 5*, 991−1000.
22. Krimm, S., and Bandekar, J. (1986) *Adv. Protein Chem. 38*, 181−364.
23. Shortle, D., and Meeker, A. K. (1986) *Proteins: Struct., Funct., Genet. 1*, 81−89.
24. Pace, C. N. (1986) *Methods Enzymol. 131*, 266−280.
25. Herrmann, L., Bowler, B. E., Dong, A., and Caughey, W. S. (1995) *Biochemistry 34*, 3040−3047.
26. Godbole, S., Dong, A., Garbin, K., and Bowler, B. E. (1997) *Biochemistry 36*, 119−126.
27. Dong, A., Huang, P., and Caughey, W. S. (1992) *Biochemistry 31*, 182−189.
28. Kauppinen, J. K., Moffatt, D. J., Cameron, D. G., and Mantsch, H. H. (1981) *Appl. Opt. 20*, 1866−1879.
29. Dong, A., and Caughey, W. S. (1994) *Methods Enzymol. 232*, 139−175.
30. Chirgadze, Y. N., Federov, O. V., and Trushina, N. P. (1975) *Biopolymers 14*, 679−694.
31. Makhatadze, G. I., Clore, G. M., and Gronenborn, A. M. (1995) *Nat. Struct. Biol. 2*, 852−855.
32. Fink, A. L., Calciano, L. J., Goto, Y., Nishimura, M., and Swedberg, S. A. (1993) *Protein Sci. 2*, 1155−1160.
33. Levitt, M., and Greer, J. (1977) *J. Mol. Biol. 114*, 181−293.
34. Torchia, D. A., Sparks, S. W., and Bax A. (1989) *Biochemistry 28*, 5509−5524.
35. Wang, J., LeMaster, D. M., and Markley, J. L. (1990) *Biochemistry 29*, 88−101.
36. Wang, J., Hinck, A. P., Loh, S. N., and Markley, J. L. (1990) *Biochemistry 29*, 102−113.
37. Wang, J., Hinck, A. P., Loh, S. N., and Markley, J. L. (1990) *Biochemistry 29*, 4242−4253.
38. Gittis, A. G., Stities, W. E., and Lattman, E. E. (1983) *J. Mol. Biol. 232*, 718−724.
39. Carra, J. H., Anderson, E. A., and Privalov, P. L. (1994) *Protein Sci. 3*, 944−951.
40. Creighton, T. E., and Shortle, D. (1994) *J. Mol. Biol. 242*, 670−680.
41. Torii, H., and Tasumi, M. (1992) *J. Chem. Phys. 96*, 3379−3387.
42. Mantsch, H. H., Perczel, A., Hollosi, M., and Fasman, G. D. (1993) *Biopolymers 33*, 201−207.
43. Shaw, R. A., Perczel, A., Mantsch, H. H., and Fasman, G. D. (1994) *J. Mol. Struct. 324*, 143−150.
44. Tiffany, L. M., and Krimm, S. (1973) *Biopolymers 12*, 575−587.
45. Surewicz, W. K., Szabo, A. G., and Mantsch, H. H. (1987) *Eur. J. Biochem. 167*, 519−523.
46. Muga, A., Mantsch, H. H., and Surewicz, W. K. (1991) *Biochemistry 30*, 7219−7224.

BI970620L